HEFAT2010
7th International Conference on Heat Transfer, Fluid Mechanics and Thermodynamics
19-21 July 2010
Antalya, Turkey

COMPARISON OF HEAT TRANSFER COEFFICIENT PER PRESSURE DROP RATIO IN SHELL-AND-TUBE HEAT EXCHANGER WITH SEGMENTAL AND HELICAL BAFFLE

R. Tasouji Azar *, S. Zeyninejad and F. Nemati
*Author for correspondence
Mechanical Engineering Department , Islamic Azad University, Ilkhchi Branch , Iran
E-mail: Tasouji@iauil.ac.ir

ABSTRACT

In this paper based on the simplified periodic model, the performance of two shell and tube heat exchangers are studied by using CFD method. Simulations are carried out to study on the shell side of two cases, one with segmental baffles and other with middle overlapped helical baffles in the angle of 40. According to periodic geometric characteristic of shell and tube heat exchangers, the simulations are conducted for one period by using periodic boundaries. All parameters of studied cases are same except the baffles geometries. It worth it to be told that for results validation, our comparisons are based on an ISI numerical study. For fixed thermal load and allowed pressure drop the heat transfer coefficient per unit pressure drop is the most meaningful comparison criterion, so comparison of cases are based on heat transfer coefficient per unit pressure drop verses same shell side mass flow rate. The result shows that the heat exchanger with segmental baffles has worse results about 80-90% lower than the case with helical baffles which shows the better performance of helical baffles. It should be mentioned that the results of this study are used to design pump around heat exchanger of Buten-1 unit in Tabriz petrochemical company.

INTRODUCTION

Over years heat exchangers have been the most useful equipment in industries area such as power plants, chemical engineering, petroleum refining, etc. Through all type of heat exchangers, shell and tube heat exchangers (STHXs) have the most widely usage and carries large amount of heat transfer per volume unit and are able to work under high pressure and large temperature differences.

For many years deferent type of baffles have been used in this equipment to improve the heat transfer and pressure drop. The most commonly used baffles, "segmental baffles" forces the shell side flow into a zigzag manner. Although this act of flow causes the high heat transfer, on the other hand increases the pressure drop on the shell side and results great pumping power requirement and electricity consuming as well. High range of dead zones and back flows and high risk of vibration failure on tube bundles are another disadvantages of mentioned baffles.

As science is developing, the design environment needs heat exchangers which use as less of the process stream Momentum as possible while producing a high enough heat transfer rate, therefore a fresh look into baffles arrangement is needed.

A new type of baffles arrangement known as helical baffles was developed in the Czech Republic for first time. A similar investigation was developed by a Norwegian group. These exchangers minimized the principal shortcoming of the conventional segmental baffles and showed better results [1].

NOMENCLATURE

A_o	[mm^2]	Heat transfer area based on outer diameter of tube
B	[mm]	Baffle pitch for helical baffle or baffle space for segmental baffle
c_p	[J/kg K]	Specific heat
D_i	[mm]	Shell inside diameter
D_1	[mm]	Tube bundle circumscribed circle diameter
d_o	[mm]	Tube outer diameter
S_{ij}		Mean rate of strain tensor
h	[W/m^2K]	Heat transfer coefficient
k		Turbulent kinetic energy
L	[mm]	Case length (length of one cycle)
M	[kg/s]	Mass flow rate
N		Tube number
Δp	[pa]	Shell side pressure drop
Re		Reynolds number
S	[mm^2]	Cross flow area at shell centre line
Δt_m	[K]	Logarithmic mean temperature difference
t	[K]	temperature
t_p	[mm]	Tube pitch
u	[m/s]	Fluid velocity

Special characters

β		Baffle inclination angle
ε		Turbulent energy dissipation
λ	[W/m.K]	Thermal conductivity
μ	[Pa.s]	Fluid dynamic viscosity
ρ	[Kg/m^3]	Fluid density
θ		Dimensionless temperature

Subscripts

s	Shell side
t	Tube side
w	wall
in	inlet
out	Outlet

The structure of this type of baffles arrangement is shown in Figure 1, which is the main concern of present study, as you see circular sector-shaped plates are arranged in a pseudo-helical baffle system and each baffle occupies one quadrant of the heat exchanger and are angled between the normal of heat exchanger's axis line and the baffles. In this paper helical baffles refer to such non continuous baffles which one of them has been designed and it is working in Tabriz petrochemical company and has shown proper results.

The most appropriate comparison between shell and tube heat exchangers is to consider both pressure drop and heat transfer at the same time, therefore in present study heat transfer coefficient per pressure drop unit for both types of heat exchangers on the shell side and at deferent mass flow rate, is discussed.

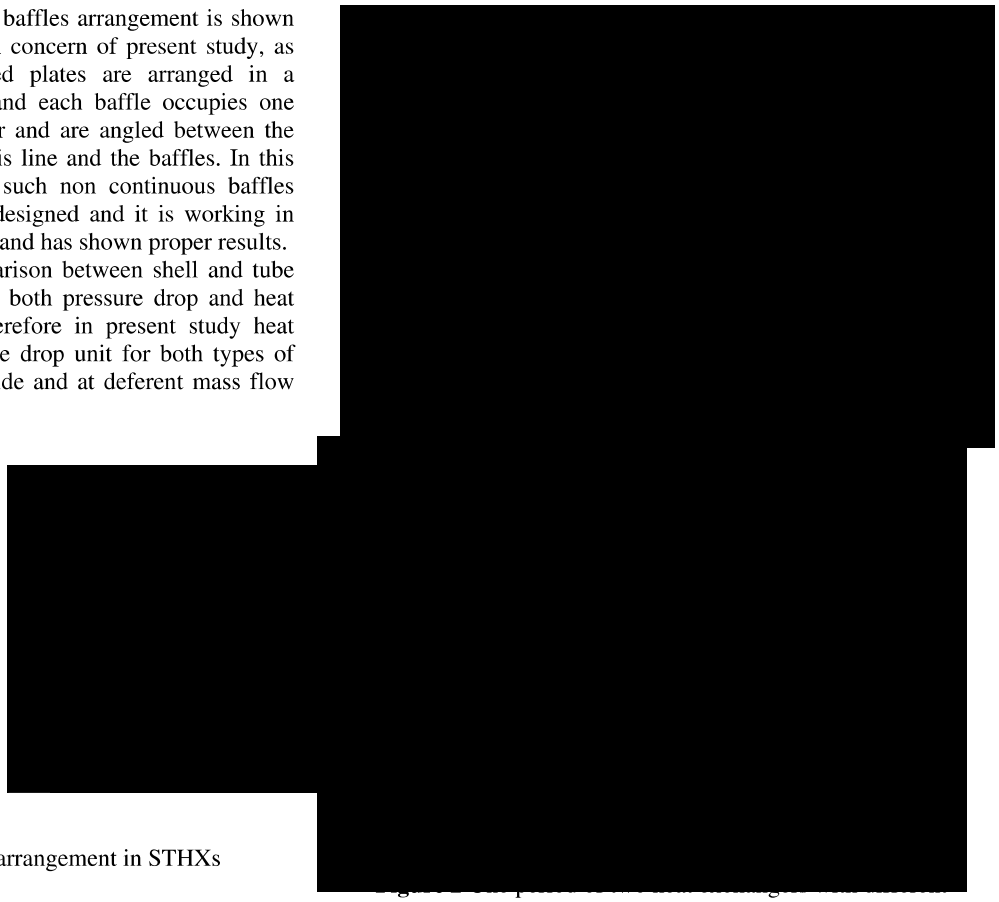

Figure 1 Helical baffle arrangement in STHXs

baffles : a) single segmental baffles. b) single-middle-overlapped helical baffles.

MODEL DISCRIPTION

In the present study the heat transfer coefficient and pressure drop on shell side of heat exchangers with two different baffle configurations are studied numerically by using CFD tool. The two configurations are: a) single-segmental baffles; and b) single-middle-overlapped helical baffles.

Due to complicated geometry of STHXs, it is difficult to acquire a reliable numerical result by simulating whole heat exchangers with a personal computer (PC). So according to the periodic geometry of STHXs, the simulations are conducted for one period of two heat exchangers by using periodic boundaries. Configurations of two heat exchangers are shown in Figure 2.

In this study all geometric parameters are assumed to be the same. The major difference is in the baffles type and configurations. Baffle inclination angle of heat exchanger with helical baffle is 40°. Based on TEMA standard cut of segmental baffles is 20%. The tube bundle arrangement is identical for two heat exchangers. More details of physical dimensions are indicated in Table 1.

The conductive-320 oil is taken as working fluid for the shell side of heat exchangers. Thermo-physical properties of the fluid are listed in Table 2.

To simplify numerical simulation the following assumptions are made in this study:

(1) Thermal properties of shell side working fluid are taken as constant. (2) The fluid flow and heat transfer processes are turbulent and in steady-state. (3) The leakage between tubes and baffles and between baffles and shell are neglected. (4) The baffles heat conduction is neglected.

Item	Value	
Shell side parameters	**Helical**	**Segmental**
D_i (mm)	211	211
L (mm)	260	260
Tube parameters		
d_o (mm)	19	19
N	37	37
Layout pattern	45°	45°
t_p (mm)	25	25
Baffle parameters		
B (mm)	250	130
β	40	0
Thickness (mm)	3	3

Table 1 Geometry dimensions of two heat exchangers

Parameter	Value
ρ (kg/m^3)	826.1
c_p (J/kgK)	2270.1
μ (kg/ms)	0.0095
λ (W/m K)	0.132

Table 2 Thermo-physical properties of fluid

GOVERNING EQUATIONS AND BOUNDARY CONDITIONS

For turbulent flow modelling the renormalization group (RNG) k-ε turbulence model [2] is adopted in this study. Compared with other models (Reynolds stress model and large-eddy simulation model) this model takes shorter computing time and less memory usage, on the other hand this model provides more accurate prediction of near wall flows [3]. The governing equations for continuity, momentum, energy, k and ε in the computational domain are shown as follows:

Continuity:

$$\frac{\partial}{\partial X_i}(\rho u_i) = 0 \tag{1}$$

Momentum:

$$\frac{\partial}{\partial X_i}(\rho u_i u_k) = \frac{\partial}{\partial X_i}\left(\mu \frac{\partial u_k}{\partial X_i}\right) - \frac{\partial \mathrm{P}}{\partial X_k} \tag{2}$$

Energy:

$$\frac{\partial}{\partial X_i}(\rho\, u_i t) = \frac{\partial}{\partial X_t}\left(\frac{k}{C_p}\frac{\partial t}{\partial X_i}\right) \tag{3}$$

Turbulent kinetic energy:

$$\frac{\partial}{\partial t}(\rho k) + \frac{\partial}{\partial X_i}(\rho k u_i) = \frac{\partial}{\partial X_j}\left(\alpha_k \mu_{eff}\frac{\partial k}{\partial X_j}\right) + G_k + \rho\varepsilon \tag{4}$$

Turbulent energy dissipation:

$$\frac{\partial}{\partial t}(\rho\varepsilon) + \frac{\partial}{\partial X_i}(\rho\varepsilon u_i) = \frac{\partial}{\partial X_j}\left(\alpha_\varepsilon \mu_{eff}\frac{\partial \varepsilon}{\partial X_j}\right) + C_{1\varepsilon}\frac{\varepsilon}{k}G_k - C^*_{2\varepsilon}\rho\frac{\varepsilon^2}{k} \tag{5}$$

Where

$$\mu_{eff} = \mu + \mu_t\,,\quad \mu_t = \rho C_\mu \frac{k^2}{\varepsilon}\,,\quad C^*_{2\varepsilon} = C_{2\varepsilon} + \frac{C_\mu \eta^3 (1-\eta/\eta_0)}{1+\beta\eta^3}$$

$$\eta = S\frac{k}{\varepsilon}\,,\quad G_k = \mu_t S^2\,,\quad S \equiv \sqrt{2S_{ij}.S_{ij}}\,,\quad S_{ij} = \frac{1}{2}\left[\frac{\partial u_i}{\partial X_j} + \frac{\partial u_j}{\partial X_i}\right]$$

Following values are the empirical constants of the RNG $k-\varepsilon$ model [3]:

$C_\mu = 0.0845$, $C_{1\varepsilon} = 1.42$, $C_{2\varepsilon} = 1.68$ $\beta = 0.012$, $\eta_0 = 4.38$

α_k and α_ε are the inverse effective Prandtl numbers for k and ε, respectively.

In shell side of STHXs, fluid flow is fully-developed, except in the primary cycles and end cycle. This is caused by influence of inlet and outlet nozzles on fluid flow in these cycles. It means that fluid flow in more cycle of STHXs is fully-developed, so simulation must be based on fully-developed fluid flow. Therefore, periodic boundary condition should be adopted on inlet and outlet boundaries to achieve the better and more reliable results. The stream wise periodically fully-developed fluid flow characteristics are indicated as follow [4]:

For fluid flow:

$$u(x,y,z) = u(x,y,z+s) \tag{6}$$
$$v(x,y,z) = v(x,y,z+s) \tag{7}$$
$$w(x,y,z) = w(x,y,z+s) \tag{8}$$
$$p(x,y,z) - p(x,y,z+s) = p(x,y,z+s) - p(x,y,z+2s) \tag{9}$$

The dimensionless fluid temperature for the periodically fully developed heat transfer with constant wall temperature is equal to:

$$\theta(\vec{r}) = \frac{t(\vec{r}) - t_{wall}}{t_{bulk\,,inlet} - t_{wall}}$$

$$T_{bulk\,,inlet} = \left(\frac{\int_A T\left|\rho\,\vec{v}.d\vec{A}\right|}{\int_A \left|\rho\,\vec{v}.d\vec{A}\right|}\right)_{inlet}$$

Where the integral is taken at the inlet section and scaled temperature (θ) obeys a periodic condition across the periodical domain as follows:

$$\theta(\vec{r},0) = \theta(\vec{r},L) \tag{10}$$

Where L is the length of one cycle.

Other boundary conditions are set as follows:
Tube wall temperature is kept constant at 300 K and upstream bulk temperature is set as 350 K. for simplifying of computation, shell wall heat transfer and baffles heat conduction are neglected. Non-slip boundary condition is applied on the all walls of heat exchangers. The standard wall function method is used to simulate the flow in viscous-sub-layers in the near-wall region.

GRID SYSTEMS

Obtaining accurate results in CFD programs need to build fine grid generation. Due to complicated structure of heat exchangers, computational domain is meshed with the unstructured Tet/Hybrid grid system. Region near tube walls are meshed with less size of cells, because of providing valid results in turbulent equations (see Figure 3). In order to ensure the accuracy of numerical results, a careful check for the grid independence of the numerical solutions was conducted. Three different grid systems are generated for two heat exchangers to obtain the optimum number of cells considering the computation time and accuracy of results (see Figure 4). It is found out that the relative deviation of average heat transfer coefficient between G2 and G3 is less than 4% for (M_s = 3.54 kg/s). So due to above results the grid system with cell number of 760,000 is used for both heat exchangers.

The governing equations are iteratively solved by the finite-volume-method with simple pressure-velocity algorithm. The iterative technique with under-relax predications of velocity and pressure is used. Default under relaxation factors of solver are employed which are 0.3, 0.7, 0.8, 0.8 and 0.9 for the pressure, momentum, turbulent kinetic energy, turbulent energy dissipation and energy, respectively. The convergence criterions are assumed to be 10^{-4} for flow field and 10^{-8} for the energy equation. For computation in this study, personal computer with CPU frequency of 4 GHz and 3 GB memory of RAM is used and each task took 10 hr for get converged solutions.

DATA REDUCTION

The major equations used in the data reduction are shown as follows:

(1) Shell side velocity and Reynolds number:

The shell side mean velocity is defined by

$$u = \frac{M_s}{\rho.S} \tag{11}$$

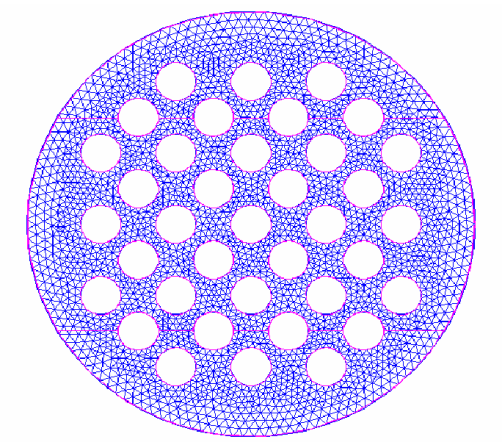

Figure 3 Front view of grid

Where (S) is the cross-flow area at the shell centre line [6]. For the non continuous helical baffles:

$$S = 0.5B\left[D_i - D_1 + \frac{D_1 - d_o}{t_p}(t_p - d_o) \right] \quad (12)$$

For the single-segmental baffles:

$$S = B\left[D_i - D_1 + \frac{D_1 - d_o}{t_p}(t_p - d_o) \right] \quad (13)$$

Where (D_i) is inside diameter of shell, D_1 is the diameter of the tube bundle circumscribed circle. For middle overlapped helical baffles (B) is baffle pitch, which defined by:

$$B = \sqrt{2}.D_i.\tan\beta \quad (14)$$

Where (β) is the baffle inclination angle. For single segmental baffles (B) is baffle spaces.

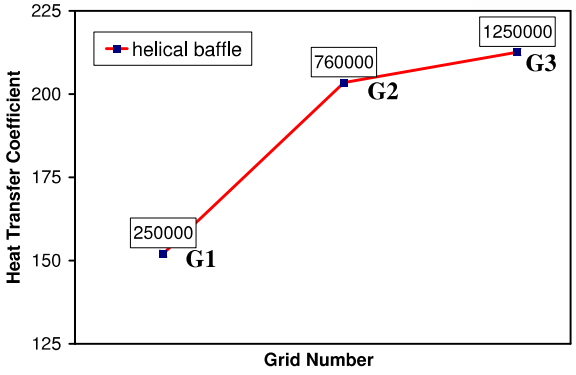

Figure 4 Independence of the numerical solutions to grid system

The Reynolds number of shell side can be calculated by [7]:

$$\mathrm{Re}_s = \frac{\rho u d_o}{\mu_s} \quad (15)$$

(2) Shell side heat transfer coefficient:

Heat transfer rate of shell side:

$$Q_s = M_s.c_{ps}.(t_{s,in} - t_{s,out}) \quad (16)$$

Shell side heat transfer coefficient is equal to:

$$h_s = \frac{Q_s}{A_o.\Delta t_m} \quad (17)$$

$$A_o = N_t.\pi.d_o.l \quad (18)$$

$$\Delta t_m = \frac{\Delta t_{\max} - \Delta t_{\min}}{\ln(\Delta t_{\max}/\Delta t_{\min})} \quad (19)$$

$$\Delta t_{\max} = t_{s,in} - t_w \quad (20)$$

$$\Delta t_{\min} = t_{s,out} - t_w \quad (21)$$

Where (t_w) is temperature of tube walls and (A_o) is the heat transfer area based on outer diameter of tubs [2].

RESULTS AND DISCUSSION

In the present study the numbers of ten cases are simulated by CFD tool due to understand the flow field and heat transfer characteristic. Performance comparison and other details are presented as follow:

1-Flow field pattern:

The flow stream lines and near-baffle velocity vectors for shell side of two heat exchangers are shown in Figure 5 and 6 respectively. As it can be seen the flow behaviour in the shell side are totally deferent.

Figure 5-a shows the flow pattern in shell side of STHX with helical baffles. As you can see the special arrangement and inclination angle of baffles force the fluid flow into a rotational manner. The fluid flow in axial direction is enhanced and the fluid flow turns into near plug flow. As it can be seen in Figures 5-a and 6-a, dead places do not occur near the helical baffles and rotational smooth motion brings about better mixing.

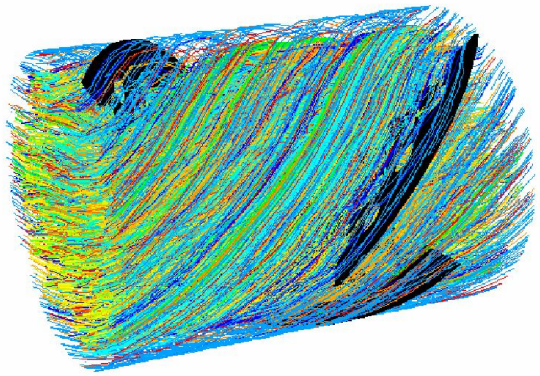

Figure 5-a The flow field pattern of helical baffle.

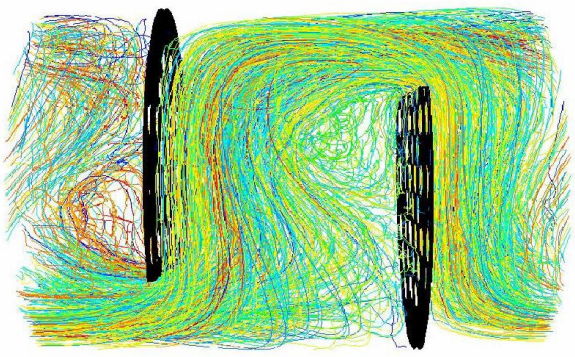

Figure 5-b The flow field pattern of segmental baffle.

Figure 6-a Velocity vectors of helical baffle.

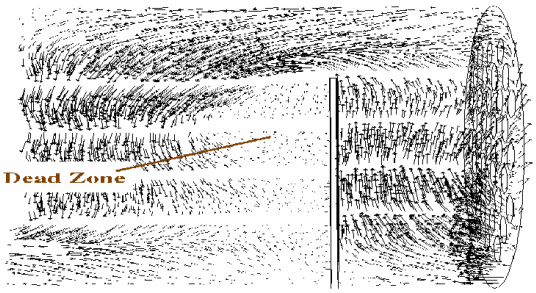

Figure 6-b Velocity vectors of segmental baffle.

As it shown in Figure 5-b and 6-b, because of the zigzag flow pattern caused by the conventional segmental baffles, there are large dead spaces and significant back mixing at the back of the baffles where fluid recalculate with low velocity and those dead zones results in inefficient use of the heat transfer area.

2-Pressure drop:

The pressure drop is an important parameter in the design of heat exchangers. Pumping costs are depended on the pressure drop therefore lower pressure drop leads to lower operation costs.

Figure 7 shows the variation of the pressure drop verses mass flow rate within (3.54 - 12 kg/s) for a segmental heat exchanger and a helical with 40° of helical angle. As you can see there is a significant deference between the results of pressure drops. For segmental baffle the flow separation at the edge of each baffles causes abrupt momentum change and serves pressure loss and also it is obvious from mentioned figure that the pressure drop increases with the increase of the mass flow rate and that increase is more evident in large mass flow rates.

3- Heat transfer coefficient:

Figure 8 reports the heat transfer coefficient verses mass flow rate, from this figure, it can be found out at the same flow rate, the shell side heat transfer coefficient of STHX with helical baffle is lower than segmental. As you can see within the tested mass flow rates, the heat transfer coefficient of helical baffle is about (34 - 50%) lower than segmental baffle. This deference can be explained by flow pattern effect. The flow pattern in the shell side of heat exchanger with segmental baffle can be regarded as cross flow which is almost normal to tube bundle but the flow pattern of helical baffle is approximately close to parallel flow so it is obvious that in the heat transfer theory, cross flow heat transfer is higher than parallel flow therefore heat transfer of segmental baffle is higher.

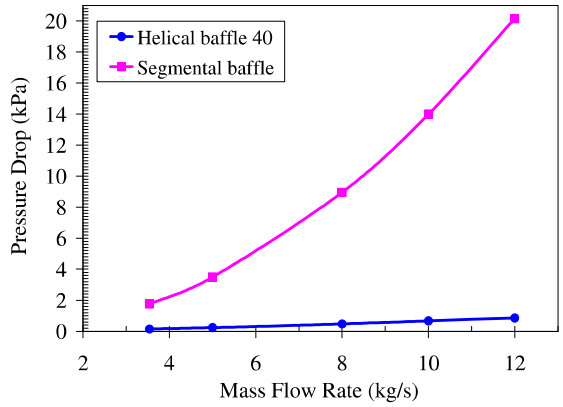

Figure 7 Pressure drop versus shell side mass flow rate for segmental and helical baffles

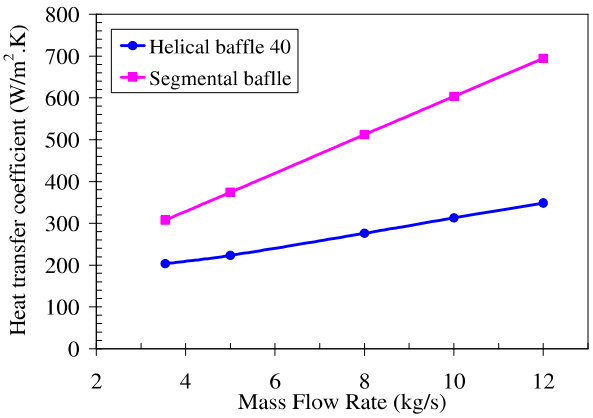

Figure 8 Heat transfer coefficient versus shell side mass flow rate for segmental and helical baffles

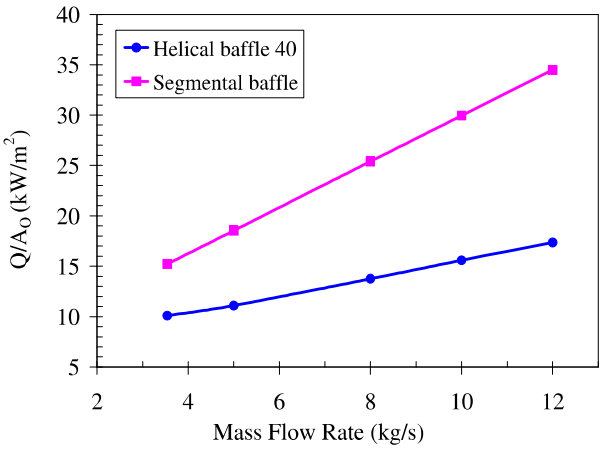

Figure 9 Heat transfer rate versus shell side mass flow rate for segmental and helical baffles

4-Heat transfer rate per Heat exchange area:

Figure 9 shows the heat transfer rate per heat exchanger area (Q/Ao). It can be obtained from mentioned figure that at The same mass flow rate (Q/Ao) for the segmental baffle is

more than helical baffle, it shows that the required area for a particular heat transfer rate is more than segmental baffle, on the other hand due to less pressure drop of helical baffle this shortcoming can be obviated by increasing mass flow rate while the pressure drop is within allowed ranges.

5-Heat transfer coefficient per pressure drop unit:

Here a very fundamental problem is remained, which one of heat exchangers structure is better? Segmental or helical?

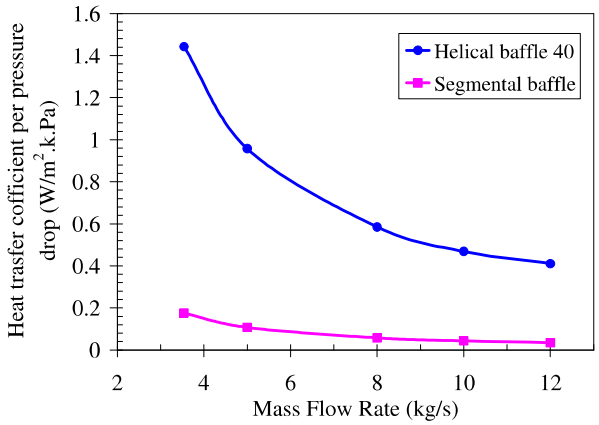

Figure 10 Heat transfer coefficient per pressure drop versus shell side mass flow rate for segmental and helical baffles

The obtained results shows that: by considering heat transfer coefficient the segmental baffle acts better and helical baffle results better by considering pressure drop.

The most meaningful compression is to compare heat transfer coefficient per pressure drop unit at the same mass flow rate (Figure 10). From this figure $h/\Delta p$ of STHX with segmental baffles is (80 - 90%) lower than STHX with helical baffles. It worth it to be mentioned this deference can be reduced almost 20% by increasing the baffle cut.

CONCLUSION:

In this paper, three-dimensional numerical simulation for heat exchangers with deferent baffle type is conducted to study the effect of baffle type on pressure drop and heat transfer coefficient. The simulations were based on two types of heat exchangers: a) segmental baffle with 20% baffle cut and b) helical baffle with inclination angle of 40°, which due to previous investigations is the optimum angle among the helix angles. The major finders are summarized as follow:

1- Under the same mass flow rate, STHXs with segmental baffles has lower pressure drop about 90% compared with segmental baffle.
2- At the same condition, STHXs with helical baffles has lower heat transfer coefficient among the other type about (34 - 50%).
3- The most important comparison of STHXs are to consider both heat transfer coefficient and pressure drop at the same time to archive the better performance of heat exchangers. Based on our study STHX with helical baffle showed significant result compared with segmental baffle.

ACKNOWLEDGMENT:

This group sincerely appreciates of all who helped specially Mr. K.Razmi a best and supportive friend.

REFERENCES

[1] P. Stehlik, Vishwas V. Wadekar, Different strategies to improve industrial heat exchange, Heat Transfer Engineering 23 (6) (2002).
[2] Jian-Fei Zhang, Ya-Ling He, Wen-Quan Tao
3D numerical simulation on shell-and-tube heat exchangers with middle-overlapped helical baffles and continuous baffles – Part II: Simulation results of periodic model and comparison between continuous and noncontinuous helical baffles, *International Journal of Heat and Mass Transfer* (2009), in press
[3] FLUENT 6.2user's guide, FLUENT Inc., 2006, section 12.4.2, section 7.5, section7.10, section 7.13.1.
[4] Yong-Gang Lei, Ya-Ling He, Pan Chu, Rui Li, Design and optimization of heat exchangers with helical baffles, *Chemical Engineering Science* 63 (2008) 4386 -- 4395
[5] K.J. Bell, Delaware method for shell side design, in: S. Kakac, A.E. Bergles, F.Mayinger (Eds.), Heat Exchangers-Thermal-Hydraulic Fundamentals and Design, Taylor & Francis, Washington, DC, 1981.
[6] Jian-Fei Zhang, Ya-Ling He, Wen-Quan Tao , 3D Numerical simulation on shell and tube heat exchangers with middle-overlapped helical baffles and continuous baffles.
Part I: numerical model and results of whole heat exchanger with middle-overlapped helical baffles, *International Journal of Heat and Mass Transfer* (2009), in press.
[7] Jian-Fei Zhang, Bin Li, Wen-Jiang Huang, Yong-Gang Lei, Ya-Ling He, Wen-Quan Tao, Experimental performance comparison of shell-side heat transfer for shell-and-tube heat exchangers with middle-overlapped helical baffles and segmental baffles, Chemical Engineering Science 64 (2009)1643-1653.